Nonequilibrium Kinetic Isotope Effects and Other Aspects of Models for HCl and DCl Elimination from Chloroethane-d_0, -d_3, and -d_5

W. G. Clark,[1] D. W. Setser,* and K. Dees

Contribution from the Chemistry Department, Kansas State University, Manhattan, Kansas 66502. Received January 7, 1971

Abstract: The nonequilibrium kinetic isotope effect for chemically activated chloroethane-d_3 and chloroethane-d_0 molecules with 91 kcal mol^{-1} of energy has been measured as 2.1. The nonequilibrium and thermal equilibrium kinetic isotope effects are in good agreement with calculated values using the RRKM formulation of unimolecular reactions and a four-centered model for the activated complex described by bond orders having the H (D) weakly bound in the ring. Recent energy-partitioning data from the literature for HF elimination from CH$_3$CF$_3$ suggest that the carbon–carbon bond order is significantly less than two at the activated complex configuration; hence, total bond order is not conserved during the HX elimination reaction. Calculated thermal unimolecular rate constants are used to illustrate the effect of pressure upon the Arrhenius activation energies for C$_2$H$_5$Cl, CD$_3$CH$_2$Cl, and C$_2$D$_5$Cl. Pressures higher than those reported in the literature are needed to deduce threshold energies from the measured Arrhenius activation energies, and the correction could affect $E_D^\circ - E_H^\circ$ by $\simeq 0.5$ kcal mol^{-1}. The influence of anharmonicity upon chemically activated nonequilibrium kinetic isotope effects was examined in model calculations; reasonable estimates of anharmonicity constants did not change the ratio of rate constants.

A s part of a continuing program[2] to provide a detailed characterization of the unimolecular four-centered HX elimination reactions of haloalkanes, we have measured the kinetic isotope effect for chemically activated CD$_3$CH$_2$Cl. Previous studies of thermal[3] and chemically activated[2b] kinetic isotope effects for the chloroethane-d_0 and -d_5 reactions, which included detailed evaluations of models using RRKM calculations, have been reported. Now results from thermal[3b] and chemical activation studies with CD$_3$-CH$_2$Cl will be used to further test the model of the transition state for the H–X elimination reactions. An interesting dependence of the difference in activation energies for C$_2$H$_5$Cl, C$_2$D$_3$H$_2$Cl, and C$_2$D$_5$Cl upon pressure, first pointed out by Lin and Laidler[4] for cyclopropane-d_0 and -d_6, is examined with the RRKM calculations.

The possible role of anharmonicity upon the magnitude of nonequilibrium unimolecular kinetic isotope effects was investigated by model calculations within the RRKM framework of unimolecular reactions. Comparison is made with experimental data for C$_2$D$_5$Cl, C$_2$D$_3$H$_2$Cl, and C$_2$H$_5$Cl.

Most of our previous studies used halogen abstraction[5] from chloro- or bromomethanes by CH$_2$-(^{1}A$_1$) as the source of the halomethyl radicals. Measurement of the ethene arising from the unimolecular decomposition of C$_2$H$_5$Cl was difficult since the CH$_2$ was generated by photolysis of ketene or diazomethane, and the reaction of CH$_2$ with these compounds gives ethene. Consequently, for the present work, mercury photosensitization[2a,6] of mixtures of CD$_3$Cl (or CH$_3$Cl) and CH$_2$Cl$_2$ was employed to generate the radicals. Decomposition and stabilization products were directly measured as a function of pressure.

Experiments with chemically activated 1,2-C$_2$H$_4$F$_2$ were done to set an upper limit on the energy partitioned to C$_2$H$_3$F. These results are compared with existing measurements of the energy partitioned to HF by the CH$_3$CF$_3$* reaction. The energy partitioning information is discussed and used to gain further insight about the four-centered structure at the barrier configuration.

Experimental Section

The experimental procedure utilizing mercury photosensitization was described previously.[2a] A droplet of Hg was added to each quartz vessel before it was filled with 2:1:0.3 parts chloromethane-d_0 or -d_3:dichloromethane:propene. Propene was added to scavenge the chlorine atoms produced by the interaction of Hg(^{3}P$_1$) with the chloromethanes.[6] This was necessary in order to prevent the decomposition product, ethene-d_2 or -h_4, from being removed by reaction with chlorine atoms. The isotopic purity of the chloromethane-d_3 was better than 99%. Vessels which were constructed from pieces of quartz tubing were attached to the vacuum line *via* a standard-taper joint. The quartz tubing was drawn out prior to filling. After transfer of the reagents and with one end of the vessel immersed in a liquid nitrogen filled dewar, the vessel was sealed under vacuum with a torch. The contents of the vessel were thoroughly mixed by shaking before being irradiated at room temperature. Depending upon the size of the vessel, the irradiation time varied from 0.25 to 2 hr. A constant volume, $\sim$3.5 cm^3, of reagents was used and the desired pressure was obtained by the proper choice of vessel volume, which was measured by filling with water. Experiments with CD$_3$Cl and CH$_3$Cl were alternated to minimize the experimental error in the determination of the isotope effect. Products of the reactions were identified by comparison with retention times of known compounds on the same gas chromatography column (6 ft of Porapak-S) and from mass spectroscopic cracking patterns. The ethene and chloroethane yields were quantitatively measured at various pressures by calibrating the response of the gas chromatograph with prepared samples which were near replicas of the irradiated experimental samples. Precautions were taken to avoid loss of C$_2$H$_4$ in gas handling.

(1) NASA Predoctoral Fellow.
(2) (a) H. W. Chang and D. W. Setser, *J. Amer. Chem. Soc.*, **91**, 7648 (1969); (b) K. Dees and D. W. Setser, *J. Chem. Phys.*, **49**, 1193 (1968); (c) R. L. Johnson and D. W. Setser, *J. Phys. Chem.*, **71**, 4366 (1967); (d) J. C. Hassler and D. W. Setser, *J. Chem. Phys.*, **45**, 3246 (1966).
(3) (a) H. Heydtmann and G. W. Volker, *Z. Phys. Chem. (Frankfurt am Main)*, **55**, 296 (1967); (b) G. W. Volker and H. Heydtmann, *Z. Naturforsch. B*, **23**, 1407 (1968); (c) H. Heydtmann, *Ber. Bunsenges. Phys. Chem.*, **72**, 1009 (1968).
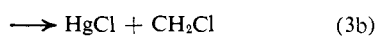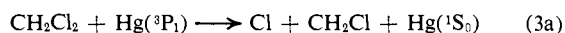(4) K. J. Laidler and M. C. Lin, *Trans. Faraday Soc.*, **64**, 927 (1968).
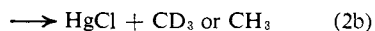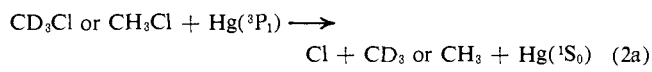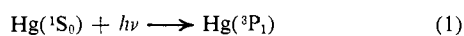(5) W. G. Clark, D. W. Setser, and E. E. Siefert, *J. Phys. Chem.*, **74**, 1670 (1970).

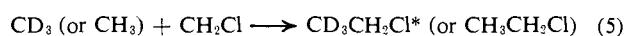(6) D. W. Setser, *J. Amer. Chem. Soc.*, **90**, 582 (1968).

The low-pressure experiments with 1,2-C$_2$H$_4$F$_2$ were done by photolysis of 1,3-difluoroacetone at room temperature with the unfiltered light of an AH-6 high-pressure lamp. Spherical Pyrex vessels ranging in size from 100 to 12000 cm^3 were used. The products were recovered by standard vacuum-line techniques and identified and measured by comparison of the retention times from gas chromatographic analyses with known samples.

Results

Reaction Mechanism and Unimolecular Rate Constants. The primary reaction initiated by the absorption of the 2537-Å Hg resonance line are given below.

$$Hg(^1S_0) + h\nu \longrightarrow Hg(^3P_1) \qquad (1)$$

$$CD_3Cl \text{ or } CH_3Cl + Hg(^3P_1) \longrightarrow$$

$$Cl + CD_3 \text{ or } CH_3 + Hg(^1S_0) \quad (2a)$$

$$\longrightarrow HgCl + CD_3 \text{ or } CH_3 \qquad (2b)$$

$$CH_2Cl_2 + Hg(^3P_1) \longrightarrow Cl + CH_2Cl + Hg(^1S_0) \quad (3a)$$

$$\longrightarrow HgCl + CH_2Cl \qquad (3b)$$

These are followed by numerous radical–radical reactions; we are concerned with the combination reactions of methyl and chloromethyl radicals.

$$2CD_3 \text{ (or } CH_3) \longrightarrow C_2D_6^* \text{ (or } C_2H_6^*) \qquad (4)$$

$$CD_3 \text{ (or } CH_3) + CH_2Cl \longrightarrow CD_3CH_2Cl^* \text{ (or } CH_3CH_2Cl) \quad (5)$$

$$2CH_2Cl \longrightarrow CH_2ClCH_2Cl^* \qquad (6)$$

The products of reactions 4–6 contain vibrational energy released from formation of the C–C bond. The chloroethanes decompose by HCl elimination unless the vibrational energy is removed by a collision.

$$CD_3CH_2Cl^* \xrightarrow{k_a} CD_2CH_2 \text{ (D)} + DCl \qquad (7)$$

$$\xrightarrow{\omega} CD_3CH_2Cl \text{ (S)} \qquad (8)$$
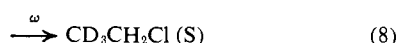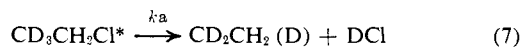
A plot of the ratio of the yield of decomposition to stabilization product vs. pressure is shown in Figure 1.

Since Cl atoms will attack the ethene produced in reaction 7, propene was added to the reaction mixture in great excess of the expected ethene yield in order to scavenge the Cl atoms. The chloropropyl radical resulting from Cl + C$_3$H$_6$ reacts by combination and disproportionation type reactions with itself and with other radicals. These products did not interfere with the analysis for chloroethane or ethene; however, they did prevent study of 1,2-dichloroethane produced in (6). Although the products associated with the reactions of C$_3$H$_6$Cl were not studied, they did constitute a large fraction of the total product yield. Undoubtedly a description of the entire reaction mechanism for all the radicals would be quite complex.[6]

Mass spectral analyses of the products from reactions 4–8 showed the expected species, i.e., ethane-d_6, chloroethane-1,1,1-d_3, and ethene-1,1-d_2. In addition to confirming that the starting reagents were of high purity, the observation of only C$_2$H$_2$D$_2$ as the elimination product shows that α,β-elimination is the only reaction pathway for CD$_3$CH$_2$Cl even at an energy of 90 kcal mol^{-1}. Volker and Heydtmann found the same result under thermal activation conditions.[3b] The α,α-elimination mechanism[7a] for haloethanes only seems to be important for 1,1-disubstituted haloethanes.[7]

(7) (a) M. J. Perona, J. T. Bryant, and G. O. Pritchard, *J. Amer. Chem. Soc.*, **90**, 4782 (1968); (b) M. J. Perona, H. W. Chang, K. C. Kim, and D. W. Setser, unpublished results.
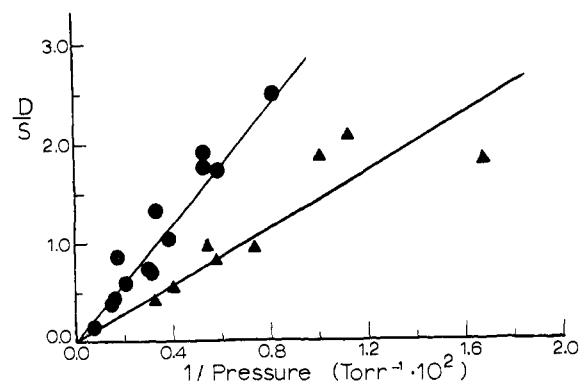

Figure 1. Ratio of decomposition and stabilization products for chloroethane-d_0, ●, and chloroethane-d_3, ▲, vs. pressure.

For an efficient deactivating gas[8] the apparent rate constant, k_a, for reaction 7 is given by $k_a = \omega([D]/[S])$; ω is the collision frequency of the excited chloroethane with the bath molecules. Since ω is directly proportional to the pressure, the slope of the [D]/[S] vs. $1/P$ plot gives k_a in pressure units; the least-squares values from Figure 1 for chloroethane-d_0 and -d_3 are k_a^H and $k_a^D = 304 \pm 82$ and 143 ± 30 Torr. Using Lennard-Jones collision cross sections,[9] the rate constants become $k_a^H = 3.4 \pm 0.9 \times 10^9$ sec^{-1} and $k_a^D = 1.6 \pm 0.3 \times 10^9$ sec^{-1}.

The experimental nonequilibrium kinetic isotope effect is given by the ratio of rate constants obtained with an *efficient* deactivating gas. The collisional efficiency for removal of energy from C$_2$H$_4$Cl$_2^*$ by CH$_3$Cl and CH$_2$Cl$_2$ has been studied,[2,5] and 8–10 kcal mol^{-1} is removed per collision. This is sufficient so that the high-pressure experimental rate constant ratio can be used as a measure of the kinetic isotope effect in the unit deactivation formulation.

The isotope effect is thus $k_a^H/k_a^D = 2.1$. For comparison, Dees measured values of 3.4 and 3.5 for chloroethane-d_3 and 1,2 dichloroethane-d_1.[2b] These isotope effects arise from a combination of primary (H/D in the four-centered part of transition state) and secondary (H/D not directly involved in the elimination reaction) effects. The contribution of the secondary effect can be obtained from $[(k_a^H/k_a^{D5})/(k_a^H/k_a^{D3})]^{1/2} = 1.27$ per deuterium atom. The primary effect can then be deduced from $(k_a^H/k_a^{D3})/(1.27)^2 = 1.29$.

The data in Figure 1 show a rather large standard deviation. The main reasons for this seemed to involve complications from the several types of radicals in the system. Apparently, large quantities of chlorine atoms are released by the primary quenching steps because the consumption of propene was high. The reaction time was kept short enough so that less than 50% of the initial propene was consumed. Since CD$_3$ (or CH$_3$) and CH$_2$Cl radicals are removed by reac-

(8) We have previously shown[2a,b] that CH$_3$Cl or CH$_2$Cl$_2$ removes 8 $\pm$ 2 kcal mol^{-1} per collision with C$_2$H$_4$Cl$_2^*$. The correction of the measured k_a values to unit deactivation efficiency is insignificant relative to the experimental uncertainty of the measurements in Figure 1.

(9) (a) J. P. Hirschfelder, C. F. Curtis, and R. B. Bird, "Molecular Theory of Gases and Liquids," Wiley, New York, N. Y., 1964, p 1212; (b) R. A. Svehla, NASA Technical Report No. R-132, Lewis Research Center, Cleveland, Ohio, 1962. (c) The product of σ and $[\Omega^{22}(T^*)]^{1/2}$ is probably a more appropriate collision diameter for collisional deactivation. Since our main interest is the isotope effect, the exact magnitude of the rate constants is not important.

Table I. Comparison of Experimental and Calculated Results

	C₂H₅Cl Exptl	C₂H₅Cl Calcd	CD₃CH₂Cl Exptl	CD₃CH₂Cl Calcd	C₂D₅Cl Exptl	C₂D₅Cl Calcd
k_a, sec^{-1}	$(3.4 \pm 0.9 \times 10^9)^a$ $(4.0 \pm 0.4 \times 10^9)^b$		$(1.6 \pm 0.3 \times 10^9)^a$		$(1.2 \pm 0.1 \times 10^9)^b$	
$\langle E \rangle$, kcal mol^{-1} ^{c}	91.0		92.0		92.5	
$E_{\min}$, kcal mol^{-1} ^{c}	88.4		89.3		89.4	
k_a, harmonic^d		2.39×10^9		1.17×10^9		8.11×10^8
$E°$, kcal mol^{-1} ^{e}	55.0^b		56.7 ± 0.5 $(56.4 \pm 0.5)^e$	56.3	56.9 ± 0.5 $(56.4 \pm 0.5)^e$	56.4
Preexponential factor,^{d,f} sec^{-1}	13.08^b	13.22	13.28^e	13.29	13.28	13.31
$[k_a^H/k_a^D]$, exptl^g			$(2.1 \pm 0.2)^a$		$(3.3 \pm 0.4)^b$	
$[k_a^H/k_a^D]$, harmonic^h				2.04		2.95
$\langle 1/D \rangle^{-1}$, cm^{-1} ^{i}		17625		17675		18266
k_a, anharmonic		1.03×10^9		5.07×10^8		3.72×10^8
$[k_a^H/k_a^D]$, anharmonic^h				2.03		2.77

^{a} This work. ^{b} See ref 2b for these values. ^{c} $\langle E \rangle$ is the average energy of the chemically activated molecules; $E_{\min}$ is the start of the distribution function. $E_{\min}$ for C₂H₅Cl was obtained from the thermochemistry previously assigned;^{2b} the values for CD₃CH₂Cl and C₂D₅Cl were obtained from the zero-point energy changes. All models of complexes, molecules, and radicals fitted the Teller–Redlich product rule to within 10%. ^{d} The calculations in this table are for a bond order specification^{11} of 1.9, 0.9, 0.1, and 0.1 for the C–C, C–Cl, Cl–H, and H–Cl bonds. The moments of inertia, the frequencies for C₂H₅Cl and C₂D₅Cl molecules, and the out-of-ring frequencies for their complexes are the same as specified in ref 2b. Only minor differences arise for the ring frequencies from Johnston's bond order specifications,^{11} e.g., k_a^H was calculated^{2b} as 2.46×10^9 sec^{-1} rather than 2.39×10^9 sec^{-1}. All models for the molecules and four-centered complex fit the Teller–Redlich product rule to within 10%. ^{e} The measured Arrhenius activation energies^3 were converted to threshold energies, $E°$, by the method described in footnote c of Table II. See the text for an analysis of the pressure dependence of the Arrhenius activation energies which suggests that the true high-pressure threshold energies are lower than those measured in ref 3; these corrected values are enclosed in parentheses. The calculated threshold energies for CD₃CH₂Cl and C₂D₅Cl were obtained from $E_H° = 55.0$ kcal and the appropriate zero-point energy changes. ^{f} The preexponential factor is in the form $(\sigma k T/h)Q_{vr}\dagger/Q_{vr}^*$; the torsional degree of freedom was treated as a hindered internal rotor in this calculation. The values in the table are for 800°K. ^{g} The experimental thermally activated isotope ratios have been measured as 1.99 and 1.87 at 712°K for C₂D₅Cl and CD₃CH₂Cl;^{3} the values calculated from models are 2.21 and 2.19, respectively. ^{h} These ratios were were obtained from $\int_{E_H°}^{\infty} k_E^H f(E)_H dE / \int_{E_D°}^{\infty} k_E^D f(E)_D dE$. ^{i} The value of $\langle D^{-1} \rangle^{-1}$ for the molecules was estimated (see text), and the same value was used for the complex.

tion with chloropropyl radicals, by combination with each other, and by H abstraction from CH₂Cl₂, the limitation on the reaction time led to small yields of desired products and scatter in the results. Two previous determinations^{2b,d} utilizing internal standard techniques gave 4.6×10^9 and 3.0×10^9 sec^{-1} as the rate constant for C₂H₅Cl*; the present error limits encompass the earlier results.

Calculated Thermal and Chemical Activation Isotope Effects. The unimolecular rate constants for C₂H₅Cl, CD₃CH₂Cl, and C₂D₅Cl were calculated using the harmonic oscillator RRKM formulation with the model^2 of the four-centered HX elimination transition state that has been shown to be satisfactory for calculating rate constants for thermally and chemically activated haloalkanes.^{10} Bond orders are assigned to the four bonds in the complex that undergo marked change. These bond orders were used to obtain stretching force constants which were combined with one-ring bending force constant to calculate the in-plane normal-mode vibrational frequencies of the four-membered ring. Off-diagonal force constants were not included. As a starting point the sum of the bond orders was assumed to be conserved during the course of the elimination reaction. The essential feature that emerged from previous work^{2b} was that the H or D must be loosely bound in the transition state in order to reproduce the observed isotope effects.

For the present calculations the model just described with bond orders^{11} of 1.9(C–C), 0.9(C–Cl), 0.1(H–C), and 0.1(H–Cl) was used. The CH₂ out-of-ring frequencies were assigned by analogy with ethene and cyclobutane; the ring puckering frequency was set to simultaneously best fit all the kinetic data. Since thermal and chemical activation data are available for C₂H₅Cl, CD₃CH₂Cl, and C₂D₅Cl and since all frequency assignments were made to fit the Teller–Redlich product rule to within 10%, very little freedom exists for arbitrary variation of the frequencies of the transition-state model. The former calculations for C₂H₅Cl and C₂D₅Cl were repeated for consistency; however, the models are essentially the same as listed by Dees and Setser.^{2b} A complete vibrational analysis^{12} of the three chloroethane isotopes has recently appeared. The frequencies are virtually identical with those used in our previous models, and these were retained for sake of consistency. All of the results are summarized in Table I; adequate agreement exists between calculated and experimental quantities. A correction to the measured Arrhenius activation energies, to be discussed below, enhances the agreement.

Vibrational Anharmonicity, the Calculated Values of k_a, and the Nonequilibrium Kinetic Isotope Effect. There have been several treatments which included vibrational anharmonicity in the RRKM formulation of the specific rate constant.^{13}

(10) A. W. Kirk, A. F. Trotman-Dickenson, and B. L. Trus, *J. Chem. Soc. A*, 3058 (1968). In their RRKM calculations these authors used a slightly different model of the activated complex for HX elimination from fluoroalkanes than the four-centered model used by Chang and Setser.^{2a} Since the magnitudes of the calculated values of k_a are not very sensitive to the individual frequencies (out of a total of 17 for C₂H₅F†), these calculations are in reasonably close agreement with results from the four-centered model.

(11) H. S. Johnston, *J. Amer. Chem. Soc.*, **86**, 1643 (1964).

(12) (a) F. A. Miller and F. E. Kivat, *Spectrochim. Acta, Ser. A*, **25**, 1363 (1969); (b) W. G. Fateley, F. E. Kivat, and F. A. Miller, *ibid.*, *Ser. A*, **26**, 315 (1970).

(13) (a) Z. Prasil and W. Forst, *J. Phys. Chem.*, **71**, 3166 (1967); (b) W. Forst and P. St. Laurent, *Can. J. Chem.*, **45**, 3169 (1967); (c) F. W. Schneider and B. S. Rabinovitch, *J. Amer. Chem. Soc.*, **84**, 4215 (1962).

Table II. Thermal Unimolecular Rate Constants for Chloroethane-d_0, -d_3, and -d_5 at 650 and 950°K

Molecule	Rate constants[c,d]	Pressure, Torr							
		10^4	10^3	10^2	10	1.0	10^{-1}	10^{-2}	10^{-3}
C_2H_5Cl[a]	$4.67 \times 10^{13} \exp(-56,400/RT)^c = 0.506\,(-5)$	0.506	0.505	0.502	0.475	0.377	0.214	0.076	0.014
CD_3CH_2Cl[a]	$5.59 \times 10^{13} \exp(-57,800/RT)^c = 0.205\,(-5)$	0.205	0.205	0.204	0.198	0.169	0.110	0.049	0.014
C_2D_5Cl[a]	$5.81 \times 10^{13} \exp(-57,900/RT)^c = 0.197\,(-5)$	0.197	0.197	0.196	0.192	0.170	0.119	0.058	0.020
C_2H_5Cl[b]	$7.56 \times 10^{13} \exp(-57,150/RT)^c = 0.530\,(1)$	0.530	0.524	0.484	0.357	0.183	0.063	0.015	0.0022
CD_3CH_2Cl[b]	$7.92 \times 10^{13} \exp(-58,340/RT)^c = 0.293\,(1)$	0.293	0.291	0.276	0.219	0.125	0.048	0.013	0.0026
C_2D_5Cl[b]	$7.96 \times 10^{13} \exp(-58,390/RT)^c = 0.285\,(1)$	0.285	0.283	0.272	0.223	0.134	0.055	0.016	0.0036

[a] Values were calculated for 650°K. [b] Values were calculated for 950°K. [c] These are "Arrhenius form" unimolecular rate constants at $P = \infty$. They were calculated from the equation $k_\infty = (\sigma kT/h)\,e^{\Delta S\dagger/R}e^{-E^a/RT}$ with E^a calculated from the $E°$ values of Table I using eq 155 from S. Glasstone, K. J. Laidler, and H. Eyring, "Theory of Rate Processes," McGraw-Hill, New York, N. Y., 1941. For these calculations the torsional mode was treated as a vibrational degree of freedom (note that the preexponential factors of Table I were calculated using a hindered internal rotor). [d] The position of the decimal is indicated by the number in parentheses.

$$k_E = \sigma Z_1 \dagger \Sigma P(E_v\dagger)/h Z_1^* N^*(E_v)$$

Anharmonicity is invoked in a conceptual way to provide coupling of the fundamental vibrational modes. In addition, anharmonicity must affect the magnitude of the calculated specific rate constant by increasing the vibrational state sums of the complex, $\Sigma P(E_v\dagger)$, and densities, $N^*(E_v)$, of the molecule. Anharmonicity affects the thermal equilibrium unimolecular rate constants in an extremely small way, and such measurements cannot evaluate the importance of anharmonicity. The anharmonic contribution to the magnitude of nonequilibrium rate constants is difficult to assess because of lack of knowledge about collision cross sections, transition state frequencies, and anharmonicity constants, as well as the computational problem of evaluating anharmonic sums and densities of states. It was hoped that these uncertainties could be reduced by examining the role of anharmonicity for the kinetic isotope effects which depend only upon the ratios of the sums and densities. The method employed to estimate the anharmonic sums and densities was formulated by Haarhoff,[14b] and has been used by Forst.[13a,b] The anharmonic constants are based upon the equation $G(v) = \omega_e \cdot (v + 1/2) - \omega_e \chi_e (v + 1/2)^2$. A recent treatment by Hoare[14c,d] uses the χ_e value for each normal mode. The formulation by Haarhoff employs an *average* Morse dissociation energy, $\langle D^{-1} \rangle = \langle \Sigma 1/D_i \rangle$ for the whole molecule. The $1/D$ value may be used as a parameter, or a mean can be found from the anharmonicity constants of the individual normal modes, using the equation $D_i = \omega_e/4\chi_e$ for each mode. The $\omega_e/4\chi_e$ anharmonic correction is appropriate for stretching vibrations; bending, wagging, and similar types of vibrations often have quite different anharmonicity expressions. Since anharmonicity constants have not been measured for most molecules and certainly are not known for activated complexes, any correction to the harmonic sums and densities is, at best, only an estimate. In addition, as Hoare and Ruijgrok[13c,d] have pointed out, even the computational methods supposedly giving correct anharmonic sums for a given set of anharmonicity constants do not agree. However, for the cyclopropane test case, most authors[14e] obtain anharmonic sums of states which are two to three times the harmonic values for energies of 80–100 kcal mol^{-1}.

For the isotopically labeled chloroethanes, the $1/D_i$ values were obtained from the anharmonicity constants $(2\chi_i = 1 - \nu_i/f_i$, where ν_i is the fundamental frequency and f_i is the harmonic frequency). ν_i and f_i, which have been measured for chloromethane,[15a] ethane,[13a] ethene,[15b] and cyclopropane,[15c] were used to assign values of $2\chi_i$ for chloroethane-d_0. In order to be consistent with the product rule, the χ_i values for the deuterated molecules were estimated using the relation[15b] $\chi_i^D/\chi_i^H = \nu_i^D/\nu_i^H$. As noted in Table I, the same value of $\langle 1/D \rangle^{-1}$ was used for the molecule and complex. Including anharmonicity lowered the calculated k_a values by about a factor of 2; similar effects have been reported by other authors.[13b] Since $\langle 1/D \rangle^{-1}$ was the same for the molecule and complex, the factor of 2 change in k_a is accounted for by the energy difference between the molecule and complex. The density of states for the molecule was calculated at 80–90 kcal, while the sum of states of the complex was calculated at 20–30 kcal. The correction factor increases with energy, so the overall effect is to decrease k_a by a factor of about 2. This factor could, of course, be altered by various assignments of $\langle 1/D \rangle^{-1}$ for the complex.

Inclusion of anharmonicity had virtually no influence upon the calculated isotope effects. This was mainly because $\langle 1/D \rangle^{-1}$ did not vary much for the three isotopically substituted molecules, at least for the method used to find χ_i and D_i.

Calculated Pressure Dependence of Arrhenius Parameters. Thermal activation experiments for various deuterated haloethanes (see Table I and ref 16) always give large, 1.5–2.0 kcal mol^{-1}, activation energy differences for the primary isotope effect. The maximum that we could obtain from our previous models was about 1.4 kcal mol^{-1}. Lin and Laidler[4] showed that the Arrhenius activation energy difference between cyclopropane-d_0 and -d_6 was pressure dependent and actually passed through a maximum at intermediate pressures. For these reasons we calculated the Arrhenius activation energies for chloroethane-d_0, -d_3, and -d_5 over a wide range of pressure. The procedure involved computing the thermal activation rate constant, k_{uni} from 600 to 950°K using the unit collision RRKM formulation with numerical integration of the

(14) (a) K. W. Wilde, *J. Chem. Phys.*, **41**, 448 (1964); (b) P. C. Haarhoff, *Mol. Phys.*, **7**, 101 (1963); (c) M. R. Hoare and Th. W. Ruijgrok, *J. Chem. Phys.*, **52**, 113 (1970); (d) M. R. Hoare, *ibid.*, **52**, 5695 (1970); (e) for a recent review, see W. Forst, *Chem. Rev.*, **71**, 339 (1971).

(15) (a) S. Reichman and J. Overend, *J. Chem. Phys.*, **48**, 3095 (1968); (b) B. N. Cyvin and S. H. Cyvin, *Acta Chem. Scand.*, **17**, 1831 (1963); (c) Hs. H. Gunthard, R. C. Lord, and T. K. McCubbin, Jr., *J. Chem. Phys.*, **25**, 768 (1956).

(16) (a) A. T. Blades, P. W. Gilderson, and M. G. H. Wallbridge, *Can. J. Chem.*, **40**, 1526 (1962); (b) A. T. Blades, P. W. Gilderson, and W. G. H. Wallbridge, *ibid.*, **40**, 1533 (1962).
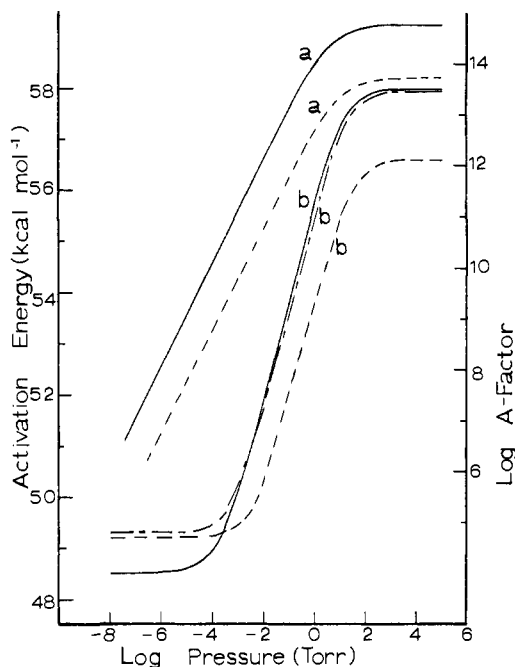
Figure 2. Calculated values of Arrhenius parameters at various pressures. (a) A factors for C_2H_5Cl, - - -, and C_2D_5Cl, ——. The A-factor curve for C_2D_5Cl has been raised 1 log unit for clarity of presentation. (b) Activation energies for C_2H_5Cl, - - - -, C_2D_5Cl, ——, and CD_3CH_2Cl, - - —.

Figure 3. The calculated difference between the Arrhenius activation energies at various pressures: $E_{d_5}{}^a - E_{d_0}{}^a$, ——; $E_{d_3}{}^a - E_{d_0}{}^a$, - - —.

rate constant equation. Some sample calculations are displayed in Table II. The next step was to plot the calculated values of the thermally activated first-order rate constants at each pressure vs. $1/T$. Such plots were linear, and the Arrhenius parameters from least-squares analysis are shown in Figure 2. This plot and Table II demonstrate that the three reactions enter their falloff regions at somewhat different pressures. As we discussed before,[2c] the Arrhenius activation energy and preexponential factor both decline with pressure; the two effects taken together tend to compensate, so the reaction appears, as measured from the magnitude of the rate constant, to enter the falloff region at lower pressures than indicated by the onset of the decline in k_{uni}. The practical result for isotopically substituted molecules is a significant pressure dependence of $E_D{}^a - E_H{}^a$, as shown in Figure 3. The ratio of Arrhenius preexponential factors also is a function of pressure; for chloroethane-d_0 and -d_5 the ratios from 10^4 to 10^{-3} Torr at every factor of 10 change in pressure are 0.87, 0.86, 0.78, 0.62, 0.50, 0.40, 0.39, and 0.41. The trend with CD_3CH_2Cl and C_2H_5Cl is similar.

In the present context the important conclusion is that the difference in activation energies is predicted to have a maximum which is significantly larger than the limiting high-pressure equilibrium value. The latter are the appropriate ones for obtaining the threshold energies, $E°$. According to Figure 3 the limiting high-pressure difference in activation energies should be 1.30 and 1.33 kcal mol^{-1}, whereas the maximum values (1 Torr) would be 1.72 and 1.98 kcal mol^{-1} for $E_{d_3}{}^a - E_{d_0}{}^a$ and $E_{d_5}{}^a - E_{d_0}{}^a$, respectively. The Arrhenius parameters were measured by Heydtmann and coworkers at 0.1–10 Torr; attempts were made to extrapolate to infinite pressure, but it is not clear that
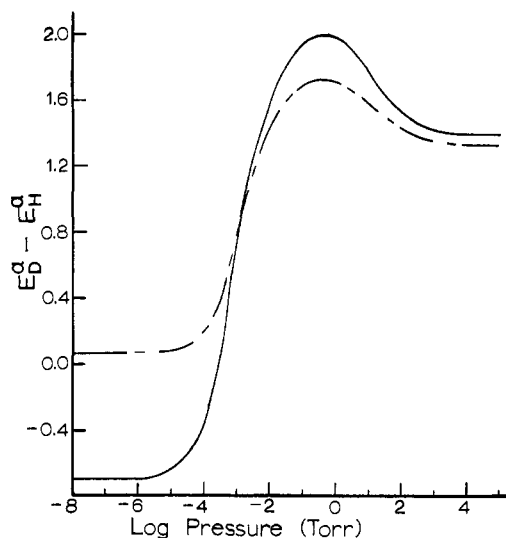
this was successful. If the predictions of Figure 3 are correct, 0.3–0.6 kcal mol^{-1} could be subtracted from the experimentally measured differences in Arrhenius activation energies. Since $E_D° - E_H°$ is virtually identical with $E_D{}^a - E_H{}^a$ for chloroethane-d_3 and -d_5 at 800°K, the corrections may be applied directly to the experimental threshold energies compiled in Table II.

The physical significance of the high-, falloff, and low-pressure parts of Figure 3 can be summarized in the following way.[17] The $E_D{}^a(\infty) - E_H{}^a(\infty)$ difference for reactions involving primary H/D isotope effects will be positive due to the zero-point energy changes. At intermediate pressures the hydrogenated molecule enters the falloff region first; consequently, $E_H{}^a$ diminishes and $E_D{}^a - E_H{}^a$ increases. The difference reaches a peak value as the deuterium-substituted molecule enters the falloff region because $E_D{}^a(\infty) - E_D{}^a(0)$ is larger than $E_H{}^a(\infty) - E_H{}^a(0)$; consequently, the change in $E_D{}^a$ with pressure is larger than for $E_H{}^a$. At limiting low pressure $E_D{}^a - E_H{}^a$ reaches a constant value which is determined by the difference in average energies of the reacting and nonreacting molecules; $(\langle E^D \rangle_r - \langle E^H \rangle_r) - (\langle E^D \rangle_n - \langle E^H \rangle_n)$. The first term is smaller at low pressure than at high pressure; consequently, $E_D{}^a(0) - E_H{}^a(0)$ is always smaller than $E_D{}^a(\infty) - E_H{}^a(\infty)$, and in some cases the low-pressure difference even becomes negative. This is unexpected at first sight since the first term is approximately $E_D° - E_H°$, which $\simeq 1.5$ kcal mol^{-1} for a primary hydrogen–deuterium isotope effect.

Discussion

Isotope Effects and the HX Elimination Reaction. As we noted earlier,[2b] the nonequilibrium isotope effects for chemically activated molecules do not provide diagnostic tests of structural changes in the reaction because of the much larger influence of the statistical isotope effect.[18] Nevertheless, the experimental non-

(17) K. M. Maloney, S. P. Pavlou, and B. S. Rabinovitch, J. Phys. Chem., 73, 2756 (1969).

(18) The very existence of this effect provided strong confirmation of the basic assumption of the RRKM theory of unimolecular reaction: B. S. Rabinovitch and D. W. Setser, Advan. Photochem., 3, 1, (1964).

equilibrium isotope effect for CD_3CH_2Cl provides a further consistency test for the models of the H(D)Cl elimination reaction. In general terms, the finding of only one isotopic ethene product and the good agreement with the computed and experimental isotope effect for chloroethane-d_3 supports the basic concept of a four-centered complex. Comparison of the rate constants for chloroethane-d_3 and -d_5 gave 1.27 as the nonequilibrium secondary isotope effect for the α-ring position. Since the nonequilibrium secondary isotope effects are quantum statistical in nature (as contrasted to zero-point energy differences for thermal activation), no measurable difference between the α or β position would be expected.

An important finding was the pressure dependence of A_H/A_D and $E_D{}^a - E_H{}^a$. With recognition of this pressure dependence, calculations now fit all rate constant data for the H (D)-X elimination reactions. In more general terms the pressure dependence of the difference in Arrhenius activation energies for deuterium-substituted molecules should be remembered whenever $E_D{}^a - E_H{}^a$ is used to obtain $E_D{}^\circ - E_H{}^\circ$, which in turn is used to define structural changes through zero-point energy arguments.

The thermal equilibrium primary isotope effect is large[16,19] (even with the correction mentioned above) and originates from the difference in threshold energies, $\sim$1.4 kcal mol^{-1}. Support for this large thermal isotope effect was the single most important factor in narrowing the choice of bond orders for describing the transition state. Within the framework of the present four-centered model, this large zero-point energy difference only can be obtained by having the hydrogen atom weakly bound to the C and Cl atoms, although not necessarily in a symmetric way. In principle the thermally activated secondary H/D kinetic isotope effects could be useful for identifying the out-of-ring structural changes since the bonding changes from sp^3 to sp^2 hybridization during the course of the reaction. Since CH_3 substitution at the α position strongly affects the threshold energies while β-substitution does not,[20] the α and β secondary isotope effects might be expected to differ. Unfortunately, the high temperature (700°K) reduces even the maximum expected effect to only 1.15 per deuterium atom for the full change from sp^3 to sp^2 hybridization.[21] Volker and Heydtmann report that $k(CD_3CH_2Cl)/k(C_2D_5Cl) = 1.01$ at 712°. Although the experiments did not utilize internal comparison, which would be highly desirable in the future, the results suggest a very small secondary isotope effect.

Nonequilibrium kinetic isotope effects are not sensitive to the inclusion of anharmonicity in the computation of sums and densities of states. Including anharmonicity gave poorer agreement between calculated and experimental nonequilibrium rate constants. Whether this is a serious defect of the RRKM theory or just an inadequate treatment of anharmonicity

and other factors affecting $N^*(E)$ and $\Sigma P(E_v\dagger)$ is an unanswered question.[22]

Improvements in the Four-Centered H–X Elimination Model. Energy-partitioning information provides an opportunity for evaluation of structural features at the barrier position as well as characteristics of the potential surface on the product side of the barrier. Recent infrared chemiluminescence[23a] and laser emission[23b] from HF generated by elimination from chemically activated CH_3CF_3 have identified the relative HF vibrational populations; $v_0:v_1:v_2:v_3:v_4:v_4 = 1.0:0.75:0.32:0.10:0.025$. Experiments in our laboratory[24] support the trend of decreasing populations for higher vibrational levels; however, our data indicate that vibrational relaxation may have affected the above ratios to some extent. Nevertheless the distribution from the *unimolecular* four-centered elimination reaction is much different from that from the *bimolecular* H-atom abstraction reaction by fluorine atoms,[25] which favor high vibrational levels of HF. Although the thermochemistry of the $CH_3CF_3{}^*$ system is somewhat uncertain, the above distribution corresponds to the release of $\sim$13% of the energy to the HF product. The initial rotational energy distribution is not known, but apparently little rotational energy is partitioned to HF. As noted by Clough, Polanyi, and Taguchi,[23a] the available energy for a chemically activated unimolecular reaction is of two types: the excess internal *kinetic* energy above the barrier and the *potential* energy released after crossing the barrier. According to the RRKM or any statistical theory, the former should be randomly dispersed in the internal modes at the barrier configuration; in contrast, the second type is released according to the potential surface in question. Clough, Polanyi, and Taguchi[23a] concluded that the potential surface for CH_3CF_3 elimination inefficiently channeled energy into HF vibration. This potential energy, 42 kcal mol^{-1} for $CH_3CF_3{}^*$, must be released to some other degrees of freedom of the products, and Clough, Polyani, and Taguchi[23a] suggested that the majority was retained as internal energy of the olefin. *Tentative* support for this conclusion was found from a study[26] of chemically activated 1,3-$C_3H_6Cl_2$ in which the product olefin apparently retained sufficient energy to undergo a second unimolecular reaction. These energy partitioning results are not consistent with a fully formed carbon–carbon double bond at the barrier configuration. The major effect from the reduction in the bond order is the lowering of one frequency from 1400 to 1000 cm^{-1}; previously published calculations[2b,d] show that such a variation in the model is of little

(19) The most recent intramolecular comparison is for CH_2DCH_2Cl;[3a] the results were not of high accuracy but a large effect, 1.7, was found at 712.5°K.

(20) (a) A. Maccoll, *Chem. Rev.*, **69**, 33 (1969); (b) G. J. Martens, M. Godfroid, and L. Ramoisy, *Int. J. Chem. Kinet.*, **2**, 123 (1970).

(21) A. Streitwieser, Jr., R. H. Jagow, R. C. Fahley, and J. Suzuki, *J. Amer. Chem. Soc.*, **80**, 2326 (1958). The estimate is based upon the change of a typical CH bending frequency from 1340 (sp^3) to 800 (sp^2) cm^{-1}.

(22) W. Forst and Z. Prasil, *J. Chem. Phys.*, **53**, 3065 (1970). The authors point out that some internal energy states are disallowed, which tends to reduce the effect of anharmonicity upon the magnitude of the rate constant. Thus, some cancellation of errors occurs in the evaluation of k_E from harmonic sums and densities.

(23) (a) P. N. Clough, J. P. Polanyi, and R. T. Taguchi, *Can. J. Chem.*, **48**, 2919 (1970); (b) M. J. Berry and G. C. Pimentel, *J. Chem. Phys.*, **49**, 5190 (1968).

(24) (a) H. W. Chang, M. J. Perona, and D. W. Setser, unpublished data; infrared chemiluminescence emission from HCl or HF produced from chemically activated chloro- and fluoroethanes supports the conclusions of ref 23a. (b) D. W. Setser, Joint Conference of the American Chemical Society and Chemical Institute of Canada, Physical Chemistry Division, May 24–29, 1970, Toronto, Canada, Abstract No. 15.

(25) (a) H. W. Chang, M. J. Perona, and D. W. Setser, *J. Phys. Chem.*, **75**, 2070 (1971); (b) R. L. Johnson, H. W. Chang, M. J. Perona, and D. W. Setser, *Chem. Phys. Lett.*, **9**, 587 (1971).

(26) K. Dees, W. G. Clark, and D. W. Setser, *J. Phys. Chem.*, **75**, 2231 (1971).
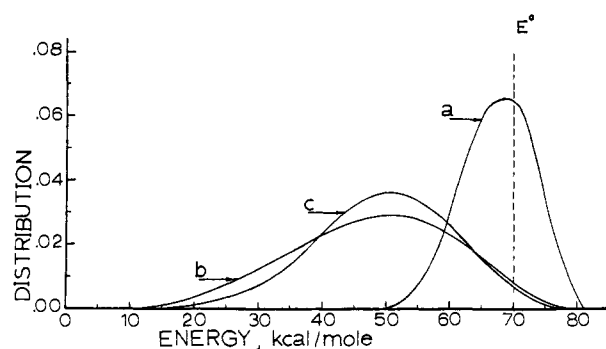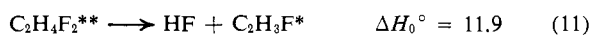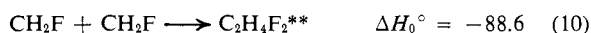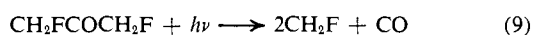
Figure 4. Some hypothetical energy distributions for $C_2H_3F^*$ formed by reaction 11; the total energy available is 80.6 kcal mol^{-1}: (a) statistical distribution of the excess energy with complete release of the potential energy to $C_2H_3F^*$, (b) statistical distribution of the excess energy with release of two-thirds of the potential energy to $C_2H_3F^*$ according to a Gaussian form with a σ of 15 kcal mol^{-1}, (c) same as (b) but with a σ of 10 kcal mol^{-1}; 70 kcal mol^{-1} is the threshold for elimination of HF from C_2H_3F.

consequence for rate constants or isotope effects of Table I. It is important to realize that special data, such as energy partitioning patterns, are necessary to identify individual microscopic features associated with unimolecular reactions of polyatomic molecules. If the carbon–carbon bond order is lowered to approximately 1 and a low bond order is maintained between H–C and H–F, a bond order sum of 3 is not conserved during the course of the reaction.

We have attempted to learn more about energy partitioning by examing the chemically activated 1,2-$C_2H_4F_2$ system at low pressure. The CH_2F radicals were generated by photolysis of 1,3-difluoroacetone and the variation of product yields were monitored as a function of pressure. The basic features of this photolysis scheme are known from the work of Pritchard and coworkers.[27]

$$CH_2FCOCH_2F + h\nu \longrightarrow 2CH_2F + CO \qquad (9)$$

$$CH_2F + CH_2F \longrightarrow C_2H_4F_2^{**} \qquad \Delta H_0^\circ = -88.6 \quad (10)$$

$$C_2H_4F_2^{**} \longrightarrow HF + C_2H_3F^* \qquad \Delta H_0^\circ = 11.9 \quad (11)$$

$$C_2H_3F^* \longrightarrow HF + C_2H_2 \qquad \Delta H_0^\circ = 15.6 \quad (12)$$

The objective was to observe the last reaction, which would identify the presence of a minimum quantity of energy in the $C_2H_3F^*$ molecule.

Unfortunately the activation energy for elimination of HF from C_2H_3F is high,[28] 70.8 ± 3.6 kcal mol^{-1}. Considering the uncertainty in the Arrhenius energy, making the minor change (1–2 kcal mol^{-1}) to a threshold energy is unnecessary. The average energy[2a] of $C_2H_4F_2^*$ at 300°K is 92.5 kcal mol^{-1}. Thus the average available energy for partitioning is 92.5 − 11.9 = 80.6 kcal mol^{-1}. Since the threshold energy for elimination of HF from 1,2-$C_2H_4F_2$ is 62 kcal mol^{-1}, the available energy can be divided into the excess energy, 30.5 kcal, and the potential energy, 50.1 kcal.

The products that were found were consistent with reactions 10 and 11. Since the competition between collisional stabilization and unimolecular decomposi-

tion of $C_2H_4F_2^*$ has been studied previously,[2a,27] this aspect was not reinvestigated. Experiments were done with pressures as low as 0.01 Torr, but no trace of acetylene could be found. All $C_2H_3F^*$ molecules with rate constants ≥ 10^5 sec^{-1} would have decomposed at 0.01 Torr. Rate constants for (12) recently have been calculated[29] (E° = 70 kcal mol^{-1}) and for even 1 kcal mol^{-1} of excess energy, the calculated rate constant is 10^6 sec^{-1}. Consequently, our experimental results show that $C_2H_3F^*$ from (11) retained less than 70 kcal mol^{-1} of energy; i.e., the internal energy of the molecules is below the threshold energy for formation of C_2H_2. We also did similar low pressure experiments with chemically activated $C_2H_4Cl_2$ molecules, which were produced by combination of CH_2Cl radicals (generated by photolysis of CH_2CO with CH_3Cl[2]). No evidence could be found for elimination of HCl from vinyl chloride.

With this information some constraints can be placed upon the energy distribution of the $C_2H_3F^*$ molecules. Two models are shown in Figure 4: (a) statistical release of the excess energy with total release of the potential energy to $C_2H_3F^*$ and (b and c) statistical release of the excess energy combined with a potential energy release represented by a Gaussian distribution centered at two-thirds of the available potential energy. The calculations are straightforward[30] and need not be described. Molecules represented by the area of the distribution that falls above the threshold energy should decompose to acetylene. The experimental fact, within the limits of our experimental sensitivity, is that all molecules contained less than the threshold energy. Thus for a Gaussian-type distribution the average potential energy released must be less than or equal to two-thirds of that available. Since the dynamics for HF elimination from 1,2-$C_2H_4F_2^*$ would be expected to resemble those of $CH_3CF_3^*$, the average HF vibrational energy can account for 10–15 kcal mol^{-1}. Hence, on the average, the relative translational and rotational degrees of freedom contain a significant fraction of the energy, although the exact amount depends on the breadth of the distribution associated with the release of the potential energy. It should be noted that formation of HF in even the v = 1 vibrational level removes 11 of the available 80.6 kcal mol^{-1}. Thus, the critical feature is the shape of the high-energy tail of the C_2H_3F distribution that corresponds to the HF molecules in the v = 0 level. Additional experimental work is needed on a haloalkane reaction for which the total energy partitioning pattern can be more completely characterized. Such information should serve to make the four-centered elimination reactions one of the most thoroughly characterized unimolecular reactions.

Conclusions

Thermal and chemical activation isotope effects provide strong evidence that the H atom is weakly bound in the four-centered ring at the barrier configuration of HX elimination reactions. Energy partitioning data based upon HX infrared chemilu-

(27) (a) G. O. Pritchard, M. Venugopalan, and T. F. Graham, J. Phys. Chem., 68, 1786 (1964); (b) G. O. Pritchard and R. L. Thommarson, ibid., 71, 1674 (1967).

(28) (a) J. M. Simmie, W. J. Quiring, and E. Tschuikow-Roux, ibid., 74, 2449 (1970); (b) E. Tschuikow-Roux, W. J. Quiring, and J. M. Simmie, ibid., 74, 992 (1970).

(29) E. Tschuikow-Roux and S. Kodama, J. Chem. Phys., 50, 5297 (1969).

(30) Y. N. Lin and B. S. Rabinovitch, J. Phys. Chem., 74, 1769 (1970).

minescence[23,24] demonstrate that surprisingly little potential energy is released as vibrational energy to HX. More tentative data[26] regarding the energy partitioned to the olefin suggest that in a large fraction, perhaps approximately two-thirds, of the potential energy may be released to the product olefin. These conclusions force an alteration of our earlier description of the carbon–carbon bond of the transition state; the bond order of ~1.8 must be modified to nearer 1.0. Such a change has little influence on the magnitude of computed rate constants or isotope effects. Analysis of the dependence of the activation energy difference for chloroethane-d_0, -d_3, and -d_5 upon pressure indicated that a maximum can occur at intermediate pressure which differs significantly from the equilibrium activation energy difference.

Molecular Order in Liquid Crystalline Solutions of Poly(γ-benzyl L-glutamate) in Dichloromethane[1]

R. D. Orwoll and R. L. Vold*

Contribution from the Department of Chemistry, University of California at San Diego, La Jolla, California 92037. Received November 23, 1970

Abstract: Poly(γ-benzyl L-glutamate) dissolved in dichloromethane forms a cholesteric liquid crystal. When allowed to come to equilibrium in a strong magnetic field, this system undergoes a slow phase transition to nematic order with polymer helix axes distributed in a narrow range about the field direction. Reorientation of polymer molecules is slow on the nmr time scale. It is shown theoretically and experimentally that this leads to a dependence of dichloromethane proton dipolar splitting on the average orientation of polymer helices with respect to the external field. This orientation can be varied by rotating the sample tube, and subsequent motion of polymer helices can be observed by following changes in the dichloromethane nmr spectrum. Dichloromethane molecules are not free to exchange rapidly between regions of sample which differ in average orientation of polymer helices.

In many lyotropic liquid crystals, long-range molecular order is produced by forces between large, nonspherical molecules dissolved in a solvent of much smaller molecules. The nature of molecular order in such systems is a topic of continuing interest, particularly in view of biological functions of lyotropic liquid crystals[2] as well as an increasing number of commercial applications of liquid crystals in general.

A number of lyotropic liquid crystals have been discovered[3,4] in which motion of the large, order-producing molecules is slow on the time scale of nuclear magnetic resonance (nmr), while the small molecules are relatively free to move about and to reorient in solution. Such systems are well suited for investigation by nmr because the small molecules exhibit more or less well-resolved dipolar splittings. Moreover, the dipolar splittings depend on the orientation of the large molecules relative to the external magnetic (or electric) field, a parameter which can be varied at will by rotating the sample tube.

We have used both the dependence of dipolar splitting on sample tube rotation and the nmr line shape to study some properties of molecular order and motion in solutions of poly(γ-benzyl L-glutamate) (PBLG) in dichloromethane. This system is particularly convenient in that the PBLG proton resonance is too wide and weak to interfere with the solvent resonance, the time scale for PBLG molecular motion varies from a few seconds to a few hours, and the line shape is not always dominated by static field inhomogeneity even for nonspinning samples.

Previous investigations[3] of dichloromethane proton resonance in PBLG solutions have demonstrated that the solution slowly undergoes a phase transition from cholesteric to nematic ordering of PBLG molecules when left in a strong magnetic field. If the sample is then rotated to some angle about an axis perpendicular to the field, its optical rotation exhibits complex behavior.[5] If a beam of polarized light is passed through the sample, it is rotated to a different extent by different regions of the sample; contorted striations are observed which move about in a complex manner for several minutes and finally disappear as the PBLG molecules become aligned along the new field direction.

In this paper we are concerned with how PBLG molecules at equilibrium in a static field produce nonzero dipolar splittings in the dichloromethane proton resonance and with the nature of molecular order and motion following a sample tube rotation.

Theory

A given dichloromethane molecule in a liquid crystal sample has at a given time t two resonance frequencies

(1) This work was partially supported by funds from the National Institutes of Health (Grant No. USPHS TRG 2-TO1-GM-01045).

(2) J. L. Fergason and G. H. Brown, *J. Amer. Oil Chem. Soc.*, **45**, 120 (1968).

(3) (a) M. Panar and W. D. Phillips, *J. Amer. Chem. Soc.*, **90**, 3880 (1968); (b) S. Sobajima, *J. Phys. Soc. Jap.*, **23**, 1070 (1967).

(4) (a) P. J. Black, K. D. Lawson, and T. J. Flautt, *Mol. Cryst. Liq. Cryst.*, **7**, 201 (1969); (b) C. S. Yannoni, private communication.

(5) W. D. Phillips, private communication.